Monolithically integrated mid-infrared sensor using narrow mode operation and temperature feedback

Daniela Ristanic, Benedikt Schwarz, Peter Reininger, Hermann Detz, Tobias Zederbauer, Aaron Maxwell Andrews, Werner Schrenk, and Gottfried Strasser

Citation: Applied Physics Letters **106**, 041101 (2015); doi: 10.1063/1.4906802
View online: http://dx.doi.org/10.1063/1.4906802
View Table of Contents: http://scitation.aip.org/content/aip/journal/apl/106/4?ver=pdfcov
Published by the AIP Publishing

Monolithically integrated mid-infrared sensor using narrow mode operation and temperature feedback

Daniela Ristanic, Benedikt Schwarz,[a] Peter Reininger, Hermann Detz, Tobias Zederbauer, Aaron Maxwell Andrews, Werner Schrenk, and Gottfried Strasser
Institute for Solid State Electronics and Center for Micro- and Nanostructures, Vienna University of Technology, Floragasse 7, Vienna 1040, Austria

(Received 3 October 2014; accepted 13 January 2015; published online 26 January 2015)

A method to improve the sensitivity and selectivity of a monolithically integrated mid-infrared sensor using a distributed feedback laser (DFB) is presented in this paper. The sensor is based on a quantum cascade laser/detector system built from the same epitaxial structure and with the same fabrication approach. The devices are connected via a dielectric-loaded surface plasmon polariton waveguide with a twofold function: it provides high light coupling efficiency and a strong interaction of the light with the environment (e.g., a surrounding fluid). The weakly coupled DFB quantum cascade laser emits narrow mode light with a FWHM of $2\,cm^{-1}$ at $1586\,cm^{-1}$. The room temperature laser threshold current density is $3\,kA/cm^2$ and a pulsed output power of around 200 mW was measured. With the superior laser noise performance, due to narrow mode emission and the compensation of thermal fluctuations, the lower limit of detection was expanded by one order of magnitude to the 10 ppm range.
[http://dx.doi.org/10.1063/1.4906802]

Mid-infrared absorption spectroscopy between 2 and 25 μm is a well established method to identify gaseous and liquid mixtures, due to fundamental rotational-vibrational absorption bands of chemical substances. Standard mid-infrared spectrometers are Fourier transform infrared spectrometers (FTIR). These are table sized instruments, commonly consisting of a broadband thermal emitter and a broadband detector, and external optics, like mirrors and lenses. They are developed to work under laboratory conditions, and the spectral resolution of the device depends on the scan length of the moving mirror. The miniaturization of sensor systems that are capable to measure small amounts of the analyte, while offering high portability, fast response, low power consumption, and low costs, pushes development in this field. The ultimate way to meet these requests will be the integration of all optical components onto a single chip. By this, the emission of the light at a specific wavelength, corresponding to the absorption peak of the target substance, and its detection take place on the same chip. In addition, the interaction of light with the target substance between the emitter and the detector must be provided.

Quantum Cascade Lasers (QCLs) are well established devices in the mid-infrared range. QCLs cover a wide emission spectrum from 2.63 μm to 250 μm.[1,2] High output power of tens of Watts in pulsed mode[3] and more than 5 W in continuous wave[4] at room temperature are reported. QCLs can provide excellent spectral quality and continuous frequency tuning.[5] Contrary to other mid-infrared coherent light sources, they emit at room temperature, have small dimensions and are cost-effective and long-lasting. All these properties make QCLs an ideal candidate for spectroscopic applications.[6–8]

On the other side, Quantum Cascade Detectors (QCDs) are reliable and stable zero bias devices that offer room temperature operation, high detection speed in the nanosecond range,[9] good noise behavior,[10] and good performance.[11] Therefore, QCDs are perfectly suited for hand-held and mobile applications. The processing technology of QCDs is fully compatible with QCLs. It was shown that the QCL material can be used as a photodetector too, but usually not at the same frequencies.[12] We have demonstrated that the coherent light source and detector, operating at the same frequencies, can be integrated on a single chip using the specifically designed heterostructure material and the same fabrication procedure.[13] This approach has the potential to serve as a basic building block of a new kind of integrated sensors.

Without any additional guiding element, the coupling efficiency drops rapidly with the distance between laser and detector, as the light is mainly emitted to free-space or to the substrate. Already for the distances longer than 20 or 30 μm, the coupling efficiency is too low for the detector to measure a reasonable signal. Dielectric-loaded surface plasmon polariton waveguides (SPPW) enable high efficiency radiation coupling between the laser and the detector and, at the same time, they serve as an interaction region.[14] The gap between the laser and the detector can be increased to 100 μm, which is sufficient to detect the absorption in liquid solutions. The introduction of the dielectric loaded SPP waveguide in the Quantum Cascade Laser/Detector (QCLD) system makes a big step towards advanced solutions in on-chip mid-infrared absorption spectroscopy. However, the resolution of the device is limited mainly due to three noise sources: mode hopping, pulse-to-pulse laser intensity, and temperature fluctuations.

If the concentration of the measured chemical substance is low, only a fraction of light will be absorbed, and the

[a]Electronic mail: benedikt.schwarz@tuwien.ac.at

alteration of the detector signal will be very small. In the pulsed regime, the laser suffers from time-dependent fluctuations of the laser output power, the optical phase, and the temporal position of the pulse.[15,16] For low concentrations of the analyte, it is difficult to distinguish if the change of the detector signal is caused by laser power fluctuations or the absorption of the analyte. Therefore, laser pulse fluctuations are recognized as a main source of noise and a sensitivity limiting factor. Laser noise can be divided into two groups: quantum noise, originating from quantum fluctuations and technical noise, coming from temperature fluctuations and pump source noise. In multimode lasers, a portion of fluctuations originates from mode hopping. A phase noise, related to the fluctuations of the optical phase, is clearly prominent in multimode lasers. For these reasons, a narrow mode emission will improve the stability of the laser intensity and thus the sensitivity of the on-chip spectrometer. The ordinary way to achieve the narrow mode emission is the implementation of a distributed feedback (DFB) grating on the top of the laser. The DFB QCLs can be designed with narrow line widths of few megahertz. They are widely used in spectroscopic applications and are often integrated in sensing devices.[17–19]

In this letter, we demonstrate a monolithically integrated lab-on-a-chip using a DFB QCL to improve the selectivity and sensitivity. Weakly coupled DFB lasers with a FWHM of $2\,\mathrm{cm}^{-1}$ are fabricated with the aim to fulfill two important tasks. First, they are spectrally narrow, taking into account that the absorption features of the liquids can be wide even up to $20\,\mathrm{cm}^{-1}$. Second, the total output power of the weakly coupled DFB QCL is comparable to a multimode emission laser, while the pulse-to-pulse intensity fluctuations are suppressed.

The inherently broad electro-luminescence spectrum of the bi-functional material used in this work spans over $200\,\mathrm{cm}^{-1}$, from 1450 to $1650\,\mathrm{cm}^{-1}$. Water at 20 °C absorbs strongly in this region and an absorption coefficient of $1145\,\mathrm{cm}^{-1}$ for the emission of $1586\,\mathrm{cm}^{-1}$ was reported.[20] The controlling liquid isopropyl alcohol has a very low absorption in this range.[21]

The bi-functional material used for the fabrication of the laser/detector structure is based on a bound-to-continuum design of 37 cascades of $In_{0.52}Al_{0.48}As/In_{0.53}Ga_{0.47}As$, lattice matched to n-doped InP substrate, grown by molecular beam epitaxy. The detailed description of the material is given elsewhere.[14]

Device fabrication started with the definition of the first order DFB grating via electron beam lithography and reactive ion etching (RIE). The grating period was chosen to be 0.96 μm (corresponds to the emission at $1586\,\mathrm{cm}^{-1}$) with a nominal grating duty-cycle of 50% and nominal grating depth of 500 nm. The 10 μm wide and 2.5 mm long lasers and 15 μm wide and 200 μm long detectors, with a gap between them of 50 μm, were etched 6 μm deep through the active zone to the substrate by RIE. 500 nm of SiN_x was deposited for electrical isolation, leaving the electrical contact area and the ridge facets towards the SPP waveguide uncovered. Layers of titanium and gold, 10 nm and 60 nm thick, respectively, were evaporated to form the SPP waveguides, providing a high quality gold surface with very low roughness. The distance between the SPP waveguides and the laser/detector facet is less than 1 μm to provide efficient light coupling. In order to minimize electric crosstalk via a shared series resistance, adjacent contacts in the trenches beside the ridges were used, instead of a standard back side substrate contact.[13] The top and bottom contacts were formed by sputter deposition of 10 nm of titanium and 250 nm of gold. On the back facets of the lasers and the detectors, a high reflection coating consisting of SiN_x and gold was applied to increase the light power and the detector absorption. The fabrication was finalized by deposition and pattering of 200 nm SiN_x used for dielectric loading of the SPP waveguide. The detector facet is intentionally designed wider than the laser facet, making the SPP waveguide tapered and increasing the coupling efficiency. As the conductivity of the liquids in our experiments is low, the electrical insulation of the completed device was not mandatory. A scanning electron microscopy (SEM) picture of the device and the DFB grating are shown in Figure 1.

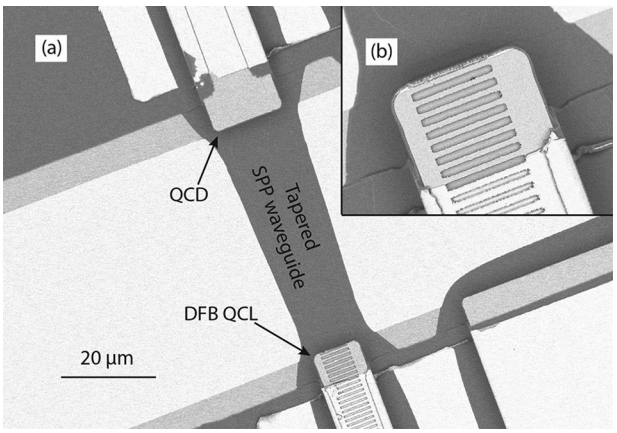

FIG. 1. (a) Scanning electron microscopy image of the monolithic mid-infrared on-chip sensor and (b) the DFB grating. Device consists of a DFB laser, a detector, and a SPP waveguide between them.

Emission spectra of the Fabry Pérot (FP) laser and the DFB laser emitting at the peak absorption frequency of the water, as well as an absorption spectrum of the detector realized in the same material, are shown in Figure 2. Spectral

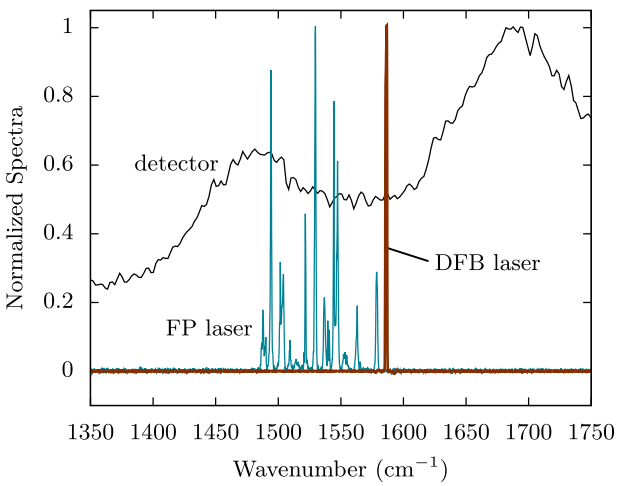

FIG. 2. Emission spectra of the narrow mode and FP lasers, as well as photocurrent spectrum of the detector. The weakly coupled DFB laser emits narrow mode with an FWHM of $2\,\mathrm{cm}^{-1}$ and a comparable output power to the multimode laser.

characterizations were performed using a FTIR spectrometer with a resolution of $0.2\,cm^{-1}$ for the lasers and $8\,cm^{-1}$ for the detector. The back facet of the laser was closed with a high reflection coating. Therefore, the light scattered from the front facet to the free-space was collected in order to measure the optical power and voltage versus current density (LIV) characteristics. The threshold current density of the laser is $3\,kA/cm^2$ (note that this is a bi-functional heterostructure). The peak optical power measured with the on-chip detector is around 200 mW, which is in the same range as for the multimode laser. The detector responsivity is 45 mA/W. All measurements were performed in pulsed mode, with a pulse length of 100 ns and a repetition rate of 5 kHz at a thermo-electrically controlled temperature of 20 °C. For such a low duty cycle operation, the thermal loading of the devices is kept low and does not influence the overall sensor performance.

During the experiments, the lab-on-a-chip device was submerged into the liquid mixture consisting of isopropyl alcohol and water, whereby the water concentration was increased over time. A magnetic stirrer was used to achieve a uniform concentration in the mixture. Real-time measurements of the voltage signal of the detector and the temperature on the chip were performed. The measurement architecture that we used in our experiments is shown in Figure 3. The signal of the on-chip detector is measured with the Boxcar Averager. The boxcar averaging allows averaging over higher number of pulses, depending on the application and requested response time, and can smooth the detector signal and contribute to its precision and accuracy. The integration time in readout circuits of the QCDs can be extended in contrast to other mid-infrared photodetectors (quantum well infrared photodetectors), due to the absence of any dark current. A prolonged integration time improves the signal-to-noise ratio (SNR) as this is proportional to the square root of the integration time. In our experiments, the averaging was applied over 5000 pulses. The gate time of 120 ns was chosen in such a manner to overlap with the laser pulses of 100 ns through the gate-width and trigger input on the box car. In this way, the signal is measured only during the laser pulsing, while the signal (noise) at all other times is unimportant and therefore neglected. If there is noise at frequencies higher than the signal frequency, it will be suppressed.

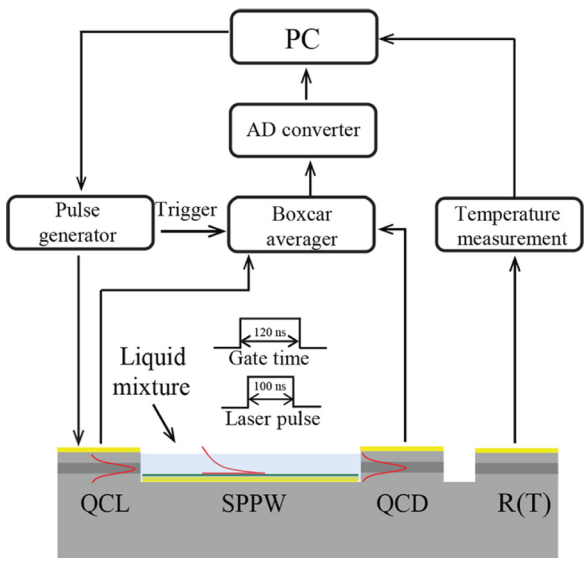

FIG. 3. An overview of the on chip sensor measurement architecture.

As the light passed through the liquid, a portion of it was absorbed by the water and the voltage signal of the detector dropped according to the Beer Lamberts law. Liquids typically have high optical background absorption. If the path length is very long, the whole optical signal may already be absorbed by the solvent and there will not be any valuable information about chemicals of interest. Therefore, the used path lengths are as short as a few micrometers. The absorption distance of 50 μm in our sensor (the gap between the laser and the detector) is sufficient for the measurement of the concentrations down to 50 ppm and provides a high dynamic range. There are many commercially available optical cells with ultra short path length of only few micrometers, suitable for the characterization of low-volume, high-absorbing substances.[22–24]

The measurement results are shown in Figure 4. The voltage signal measured on the on-chip detector is depicted in black. The detector signal changes instantaneously with the change in the concentration of the absorbing liquid. It also follows counter temperature fluctuations. In order to measure them, we used the fact that the resistance of the bi-functional heterostructure is temperature dependent. The on-chip resistive temperature sensor, mounted on the heterostructure, measured the temperature fluctuations using a Keithley 2600 Sourcemeter and they are displayed as a red line. In contrast to an external temperature sensor attached to the copper submount, the on-chip temperature sensor measurements show a strong anticorrelation of the device temperature and the detector signal. These variations can be eliminated during postprocessing. This is shown as a blue line whereby the undesired and accidental temperature fluctuations are extracted from the original voltage signal. As the referent liquid (isopropyl alcohol) evaporates faster than water and the absorption of the water from atmosphere into

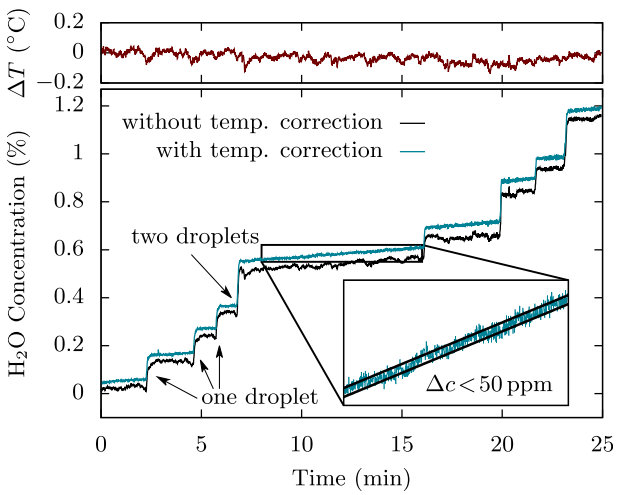

FIG. 4. Real-time on chip absorption measurement. The voltage signal on the detector is shown in black. The temperature fluctuation measured using on chip resistive temperature sensor in depicted in red. The blue line represents the corrected detector signal where the temperature fluctuations are removed from the original signal. The inset shows an enlarged view of the refined signal. Without further averaging, the fluctuations remain within a range of approximately 50 ppm.

the mixture is possible, the concentration of the absorbing liquid and the amount of absorbed light increase with time and thus the signal on the detector decreases (see inset in Figure 4).

In this paper, we demonstrated an efficient and reliable way to improve the monolithically integrated mid-infrared lab-on-a-chip. Using DFB lasers, the absorption peaks of analyte can be precisely targeted enhancing the selectivity of the sensor. The DFB QCL improves the stability of the laser intensity and thus the sensor sensitivity. By eliminating temperature fluctuations, the range of detection can be increased by an order of magnitude, down to the 10 ppm range.

With an array of DFB lasers on the same chip, the chemical content of the mixture would be measurable. The advanced measurement approaches enable extended integration times and averaging over a larger number of pulses contributing significantly to improve accuracy of the measured values. As the lower limit of detection (LOD), which determines the lowest measurable concentration, increases with the interaction length according to Beer Lamberts law, a device with an extended gap may improve the sensor sensitivity further.

The authors thank Anton Tsenov for his support and access to the electron beam lithography. This work was supported by the Austrian Science Funds (FWF) in the framework of the Doctoral School Building Solids for Function (Project W1243) and the project NextLite F4909-N23, as well as, by the PLATON project 35N within the Austrian NANO initiative and by the FP7 EU-project ICARUS (FP7-SEC-2011-285417).

[1]C. Walther, M. Fischer, G. Scalari, R. Terazzi, N. Hoyler, and J. Faist, Appl. Phys. Lett. **91**, 131122 (2007).
[2]O. Cathabard, R. Teissier, J. Devenson, J. C. Moreno, and A. N. Baranov, Appl. Phys. Lett. **96**, 141110 (2010).
[3]P. Q. Liu, A. J. Hoffman, M. D. Escarra, K. J. Franz, J. B. Khurgin, Y. Dikmelik, X. Wang, J.-Y. Fan, and C. F. Gmachl, Nat. Photonics **4**, 95 (2010).
[4]Y. Bai, N. Bandyopadhyay, S. Tsao, S. Slivken, and M. Razeghi, Appl. Phys. Lett. **98**, 181102 (2011).
[5]Y. Yao, A. J. Hoffman, and C. F. Gmachl, Nat. Photonics **6**, 432 (2012).
[6]S. S. Kim, C. Young, and B. Miziakoff, Anal. Bioanal. Chem. **390**(1), 231 (2008).
[7]A. Kosterev, G. Wysocki, Y. Bakhirkin, S. So, R. Lewicki, M. Fraser, F. Tittel, and R. Curl, Appl. Phys. B **90**, 165 (2008).
[8]A. Goyal, T. Myers, C. A. Wang, M. Kelly, B. Tyrrell, B. Gokden, A. Sanchez, G. Turner, and F. Capasso, Opt. Express **22**, 14392 (2014).
[9]D. Hofstetter, M. Graf, T. Aellen, J. Faist, L. Hvozdara, and S. Blaser, Appl. Phys. Lett. **89**, 061119 (2006).
[10]H. Schneider, P. Koidl, F. Fuchs, B. Dischler, K. Schwarz, and J. D. Ralston, Semicond. Sci. Technol. **6**, C120 (1991).
[11]P. Reininger, B. Schwarz, H. Detz, D. MacFarland, T. Zederbauer, A. M. Andrews, W. Schrenk, O. Baumgartner, H. Kosina, and G. Strasser, Appl. Phys. Lett. **105**, 091108 (2014).
[12]D. Hofstetter, M. Beck, and J. Faist, Appl. Phys. Lett. **81**, 2683 (2002).
[13]B. Schwarz, P. Reininger, H. Detz, T. Zederbauer, A. M. Andrews, W. Schrenk, and G. Strasser, Sensors **13**, 2196 (2013).
[14]B. Schwarz, P. Reininger, D. Ristanić, H. Detz, A. Maxwell Andrews, W. Schrenk, and G. Strasser, Nat. Commun. **5**, 4085 (2014).
[15]A. A. Kosterev, R. F. Curl, F. K. Tittel, R. Köhler, C. Gmachl, F. Capasso, D. L. Sivco, and A. Y. Cho, Appl. Opt. **41**, 573 (2002).
[16]U. K. R. Paschotta and H. R. Telle, in *Solid State Lasers and Application*, edited by A. Sennaroglu (CRC Press, 2007).
[17]Y. Bakhirkin, A. Kosterev, R. Curl, F. Tittel, D. Yarekha, L. Hvozdara, M. Giovannini, and J. Faist, Appl. Phys. B **82**, 149 (2006).
[18]Y. Ma, R. Lewicki, M. Razeghi, and F. K. Tittel, Opt. Express **21**, 1008 (2013).
[19]X. Wang, S.-S. Kim, R. Robach, M. Jetter, P. Michler, and B. Mizaikoff, Analyst **137**, 2322 (2012).
[20]D. M. Wieliczka, S. Weng, and M. R. Querry, Appl. Opt. **28**, 1714 (1989).
[21]See webbook.nist.gov for the absorption spectrum of isopropyl alcohol.
[22]See www.perkinelmer.com for the spectroscopy flow-through cell, Product No. B0631085.
[23]See www.specac.com for the variable pathlength liquid cell for IR spectrometry, product No. GS07500.
[24]See www.shimadzu.com for the fixed liquid cell for FTIR with 100 μm thickness.